

1 **Brown carbon aerosols from burning of boreal peatlands:**  
2 **Microphysical properties, emission factors, and implications**  
3 **for direct radiative forcing**

4 **R. K. Chakrabarty<sup>1</sup>, M. Gyawali<sup>2</sup>, R. L. N. Yatavelli<sup>2,3</sup>, A. Pandey<sup>1</sup>, A. C. Watts<sup>2</sup>, J.**  
5 **Knue<sup>2</sup>, L.-W. A. Chen<sup>2,4</sup>, R. R. Pattison<sup>5</sup>, A. Tsibart<sup>6</sup>, V. Samburova<sup>2</sup>, and H.**  
6 **Moosmüller<sup>2</sup>**

7 [1] Aerosol Impacts and Research (AIR) Laboratory, Department of Energy,  
8 Environmental and Chemical Engineering, Washington University in St. Louis, St. Louis,  
9 MO 63130, USA

10 [2] Desert Research Institute, Nevada System of Higher Education, Reno, NV, 89512,  
11 USA

12 [3] California Air Resources Board, El Monte, CA 91731, USA

13 [4] Department of Environmental and Occupational Health, University of Nevada Las  
14 Vegas, Las Vegas, NV 89154, USA

15 [5] United States Forest Service, Pacific Northwest Research Station, Anchorage, AK  
16 99501, USA

17 [6] Department of Landscape Geochemistry and Soil Geography, Moscow State  
18 University, Moscow, Russian Federation

19 Correspondence to: R. K. Chakrabarty ([chakrabarty@wustl.edu](mailto:chakrabarty@wustl.edu))

20 **Abstract**

21 The surface air warming over the Arctic has been almost twice as much as the global average in  
22 recent decades. In this region, unprecedented amount of smoldering peat fires have been

23 identified as a major emission source of climate-warming agents. While much is known about  
24 greenhouse gas emissions from these fires, there is a knowledge gap on the nature of particulate  
25 emissions and their potential role in atmospheric warming. Here, we show that aerosols emitted  
26 from burning of Alaskan and Siberian peatlands are predominantly brown carbon (BrC)—a class  
27 of visible light absorbing organic carbon (OC)—with negligible amount of black carbon content.  
28 The average fuel-based emission factors for OC aerosols ranged from 3.8 to 16.6 g.kg<sup>-1</sup>. Their  
29 mass absorption efficiencies were in the range of 0.2-0.8 m<sup>2</sup>g<sup>-1</sup> at 405 nm (violet) and dropped  
30 sharply to 0.03-0.07 m<sup>2</sup>g<sup>-1</sup> at 532 nm (green), characterized by a mean Ångström exponent of ≈9.  
31 Electron microscopy images of the particles revealed their morphologies to be either single  
32 sphere or agglomerated “tar balls”. The shortwave top-of-atmosphere aerosol radiative forcing  
33 per unit optical depth under clear-sky condition was estimated as a function of surface albedo.  
34 Only over surfaces with albedo greater than 0.6, such as snow cover and low-level clouds, the  
35 emitted aerosols could result in a net warming (positive forcing) of the atmosphere.

## 36 **1 Introduction**

37 Boreal and Arctic ecosystems store large amounts of carbon, between one-fifth and one-third of  
38 the planet’s terrestrial organic carbon, in peatlands, moss, and litter (Gorham, 1994; Turetsky et  
39 al., 2015). Carbon accumulation in this ground-layer biomass has been occurring over hundreds  
40 to thousands of years, and plays an important role in regulating the planetary carbon cycle and  
41 climate. These ecosystems act as a sink for carbon emissions from natural and human activities  
42 (Bonan, 2008). However, during the past several decades, substantial smoldering combustion of  
43 this ground-layer biomass has caused positive climate feedback by releasing stored carbon into  
44 the atmosphere as greenhouse gases and particulate matter (Oris et al., 2013; Turetsky et al.,  
45 2015). These low-temperature fires have contributed to changes in the quantity of seasonal snow

46 cover, ice and permafrost, and vegetation productivity in the Arctic Tundra, which has seen a rise  
47 in surface air temperatures at approximately twice the global rate (Hu et al., 2010; Jorgenson et  
48 al., 2001; Lawrence and Slater, 2005; Pearson et al., 2013).

49 In continental North America Boreal regions, the mean annual burn area has more than doubled  
50 in the past several decades (Oris et al., 2013). In Siberia, an average of 4 million hectares of  
51 peatlands burned annually between 1975 and 2005, with the frequency of fires doubling since the  
52 1990s (Conard and Ivanova, 1997; Sheng et al., 2004; Stocks et al., 1998). Siberia is home to  
53 about 50 percent of world's peatlands; it is anticipated that burning of these peatlands will  
54 increase by as much as 100% in the coming years in response to climate change (Bachelet et al.,  
55 2005; Balshi et al., 2009; Flannigan et al., 2005). Climate change would result in drying and  
56 lowering of the water table in peat lands, which in turn would increase the frequency and  
57 intensity of peat fires (Turetsky et al., 2015)

58 Past studies have estimated that carbon released from boreal forest fires is mostly composed of  
59 greenhouse gasses—CO<sub>2</sub>, CO, and CH<sub>4</sub> (Oris et al., 2013; Simpson et al., 2011). Past field  
60 observations and laboratory studies have also shown burning of peat lands—both tropical and  
61 boreal—to emit large quantities of greenhouse gases (Christian et al., 2003; Iinuma et al., 2007;  
62 Page et al., 2002; Stockwell et al., 2014; Turetsky et al., 2015). While much is known about  
63 gaseous emissions, properties and climatic impacts of particulate matter (or, aerosol) from these  
64 fires are poorly quantified. Black carbon (BC) aerosol has been identified as the major light-  
65 absorbing and warming agent, influencing direct radiative forcing by as much as  $17 \pm 30 \text{ W/m}^2$   
66 after a flaming boreal fire (Oris et al., 2013; Randerson et al., 2006). Emitted organic carbon  
67 (OC) aerosols from these fires have, until recently, been assumed to be purely scattering in the  
68 visible spectrum. Very little is known about the radiative effects of aerosols emitted from

69 smoldering combustion, which is the more dominant and long-lasting fire phase for boreal  
70 peatlands (Eck et al., 2009; Turetsky et al., 2015). Smoldering combustion of peatlands is an  
71 important emission source as it may emit up to six times more aerosol mass concentration per  
72 unit carbon combusted compared to flaming grassland fires (Page et al., 2004).

73 The objective of this laboratory study is to address this knowledge gap by reporting the physical,  
74 chemical, and spectrally-resolved optical properties of aerosols emitted from the laboratory  
75 combustion of peatland samples collected from interior Alaska and western Siberia. The emitted  
76 smoke aerosols were analyzed *in situ* for their spectral optical properties using multi-wavelength  
77 integrating photoacoustic-nephelometers (IPNs) and size and morphology using a scanning  
78 mobility particle analyzer (SMPS) and electron microscopy, respectively. The aerosols were  
79 simultaneously collected on quartz-fiber filters for the quantification of mass by gravimetry and  
80 carbon mass fractions using a thermal/optical carbon analyzer. With the knowledge of their  
81 optical properties, the potential warming impacts of the emitted smoke aerosols on the  
82 atmosphere were estimated using a simple forcing efficiency model integrated over the  
83 tropospheric solar spectrum.

## 84 **2 Methods**

85 Experiments were conducted during summer 2014 in the biomass combustion chamber of the  
86 Desert Research Institute (Tian et al., 2015). This aluminum chamber measures 1.83 m by 1.83  
87 m by 2.06 m high and facilitates burning of up to 50 g of solid biomass fuels under controlled  
88 conditions of temperature, dilution, and relative humidity. For this study, samples of black  
89 spruce peatlands, collected from the closed-crown boreal forests of interior Alaska and west  
90 Siberia (see details in the Supplement), were burned at two moisture content levels—25 and 50%.  
91 Previous studies have reported that peat mass loss upon ignition is highest for moisture content

92 levels below 100% (Rein et al., 2008). Prior to burning, organic soil samples were analyzed  
93 using the Flash EA 1110 analyzer (Thermo Nicolet Corporation, Waltham, USA) (Xu et al.,  
94 2011) for their carbon (C), hydrogen (H), nitrogen (N), sulphur (S), and oxygen (O) content.  
95 Based on the dynamic flash combustion method, this instrument utilizes two reaction chambers,  
96 gas chromatographic column, and thermal conductivity detector to quantify the mass fraction of  
97 C, H, N, S, and O. The fuel moisture content of the burned samples was determined by  
98 measuring the mass loss after maintaining the sample at a temperature of 90°C overnight. Fuels  
99 were prepared for combustion by arranging them in a round “pie” shape in an insulated  
100 containers to simulate “real world” conditions in which surrounding unburned peat soils provide  
101 insulation near the burn location.

102 Multiple runs (three per fuel per moisture content) of smoldering combustion of approximately  
103 20 g of Alaskan and Siberian peatland samples were conducted on a continuously weighed flat  
104 fuel bed located in the chamber. Each run lasted for about an hour. Aerosol from the smoke-  
105 filled chamber was sampled through a PM<sub>2.5</sub> (particulate matter less than 2.5 μm aerodynamic  
106 diameter) inlet and distributed via a manifold to a suite of instruments, namely a sampling unit  
107 for collecting particles onto pre-baked 47-mm diameter quartz fiber filters (Whatman, USA), a  
108 sampling unit for collecting particles for electron microscopy and analysis (Ted Pella Inc.), a 3-  
109 wavelength (405nm, 532nm, and 781 nm) IPN (Droplet Measurements Inc.) and a custom-made  
110 single wavelength (870 nm) IPN (Abu-Rahmah et al., 2006; Arnott et al., 1999; Lewis et al.,  
111 2008a), a SMPS (TSI Inc.), a non-dispersive infrared CO gas analyzer (Testo Inc.), a NO<sub>x</sub>  
112 analyzer (2B Technologies Inc.), and a CO<sub>2</sub> gas analyzer (SBA-5; PP Systems Inc.). Conductive  
113 tubing was used to transport the particles to the various instruments in order to minimize particle  
114 losses.

115 An IPN consists of a wavelength-specific laser module and a reciprocal integrating nephelometer  
116 aligned in an acoustic resonator. The instrument measures particle light absorption coefficient  
117 ( $\beta_{\text{abs}}$ ) using the photoacoustic effect (Arnott et al., 1999), while the reciprocal integrating  
118 nephelometer measures the integrated (over  $\sim 4\pi$ ) scattering from the sample volume yielding  
119 the scattering coefficient ( $\beta_{\text{sca}}$ ) (Abu-Rahmah et al., 2006). The four wavelength IPNs used in  
120 this study facilitated simultaneous measurement, with two-second time resolution, of spectrally-  
121 varying  $\beta_{\text{abs}}$  and  $\beta_{\text{sca}}$  in addition to intensive aerosol optical properties such as single scattering  
122 albedo (SSA) and Absorption Ångström Exponent ( $\alpha$ ). The SMPS was operated with a  
123 sheath/aerosol flow ratio of 10:1 (sheath flow = 3 L/min; aerosol flow = 0.3 L/min), yielding a  
124 differential mobility analyzer size transmission width of approximately  $\pm 10\%$ . The CO and CO<sub>2</sub>  
125 gas concentrations were continuously measured and the data were averaged over 5-minute  
126 intervals.

127 For each run, aerosols were collected on 47 mm quartz-fiber filters at 10 l min<sup>-1</sup> flow rate.  
128 Immediately after sampling, filters were stored in a refrigerator and later analyzed for BC and  
129 OC mass fractions and concentrations using the IMPROVE-A TOR and TOT analyses method  
130 (Chow et al., 2007; Chow et al., 2011) implemented on a DRI Model 2001 thermal/optical  
131 carbon analyzers (Atmoslytic, Inc., Calabasas, CA, USA). The fuel-based emission factor (see  
132 details in the Supplement), defined as the mass of a compound released per mass of fuel  
133 consumed (Chen et al., 2007), of BC and OC corresponding to each sampled filter were  
134 determined using the procedure described by Chen *et al.* (Chen et al., 2007). With the knowledge  
135 of OC mass concentrations and  $\beta_{\text{abs}}$ , the OC mass absorption efficiency (MAE, also referred to as  
136 mass absorption cross section) was calculated in order to highlight the mass absorption

137 contribution by OC, a parameter often ignored in aerosol forcing calculations by climate models  
138 (Chung et al., 2012; Gustafsson et al., 2009; Solomon et al., 2007; Stocker et al., 2013).

### 139 **3 Results and Discussion**

140 The mean carbon (C) dry mass fractions of the Alaskan and Siberian peat samples were  
141 estimated at  $38.1 \pm 1\%$  and  $49.6 \pm 0.2\%$ , respectively. This carbon mass predominantly converts  
142 to CO<sub>2</sub>, CO, and carbon aerosol upon combustion, thereby allowing the estimation of fuel-based  
143 EFs for BC and OC. Previous studies (Christian et al., 2003; Iinuma et al., 2007) measured  
144 slightly higher C mass fractions at 44 - 54.7% and 50.7%, respectively, for peat collected from  
145 the Sumatran region of Indonesia and the Neustädter Moor, Germany. One could qualitatively  
146 reason that past fire history and depth of sample collection may have caused this spread in C  
147 mass fractions values.

148 Table 1 summarizes the study-averaged, fuel-based EF values of CO<sub>2</sub>, CO, BC, and OC emitted  
149 from the combustion of two types of peatland samples at 25 and 50% moisture content levels.  
150 Inter-sample variability of measured EF values was small, owing mainly to use of standard  
151 amount of fuels and the nearly identical, smoldering-dominated fire patterns. The fuels burned  
152 with a modified combustion efficiency (MCE)—defined as the amount of carbon released as CO<sub>2</sub>  
153 divided by the amount of C released as CO<sub>2</sub> plus CO (Ward et al., 1996)—of  $MCE \leq 0.7$ ,  
154 indicating pure smoldering combustion. The particulate matter mass emissions during all peat  
155 burns were completely dominated by OC. Visually the smoke appeared whitish in color with no  
156 tinge of blackness (blackness would be indicative of flaming phase). The average OC EFs (per  
157 fuel mass) for Alaskan and Siberian peats ranged from 3.8 to 7 g kg<sup>-1</sup> and 9.2 to 16.6 g kg<sup>-1</sup>,  
158 respectively. This range of values is consistent with values measured for German and Indonesian  
159 peat burns, 6- 12.8 g kg<sup>-1</sup> (Iinuma et al., 2007). The average OC/BC mass ratios ranged between  
160 70 and 85 for combustion of Siberian peat and between 23 and 72 for Alaskan peat. These values

161 are much higher than the average mass ratios of 14 and 13 for combustion of Indonesian and  
162 German peat, respectively. The EF values for BC emitted from combustion of Alaskan peat  
163 ranged from 0.09 to 0.16 g kg<sup>-1</sup>, while those from Siberian peat were 0.09 to 0.23 g kg<sup>-1</sup>. This  
164 range of values is lower than previous findings of 0.04 – 1 g kg<sup>-1</sup> for BC EFs measured for  
165 combustion of Indonesian and German peat. The CO<sub>2</sub> and CO EFs were in the range of 1432 –  
166 1700 g kg<sup>-1</sup> and 50 – 204 g kg<sup>-1</sup>, respectively. The observed range is in line with previous  
167 estimates of mean CO<sub>2</sub> EF of 1616±180 g/kg and CO EF of 113±72 g/kg from boreal forest fires  
168 (Oris et al., 2013). In our study, the effects of fuel moisture on OC and BC EFs were  
169 inconclusive. For the Siberian peat samples, the OC/EC ratios were observed to increase with  
170 increasing moisture content, while for Alaskan peat samples, the opposite trend was observed.  
171 With increasing fuel moisture, OC EFs were observed to increase, while BC EF increases for  
172 Alaskan but decreases for Siberian.

173 Figure 1 shows transmission electron microscopy (TEM) images of typical particles emitted  
174 from the combustion of Alaskan and Siberian peat samples. Two basic particle shapes that were  
175 identified are: spherical and agglomerates of spherical shapes. The internal structure of the  
176 particles was amorphous in nature, which suggested that they belong to the category of “tar  
177 balls” (Chakrabarty et al., 2010; Laskin et al., 2015). This was further corroborated by the semi-  
178 quantitative Electron Dispersive Spectroscopy (EDS) analysis results of these particles, which  
179 showed a very high molar fraction of C and an average molar C-to-O ratio ranging between 6  
180 and 7. This ratio is consistent with those reported by previous studies on tar balls (Chakrabarty  
181 et al., 2006; Pósfai et al., 2003). Carbon molar fractions were larger than 80% in over 90% of  
182 the particles analyzed. It is interesting to note that a significant fraction (~60%) of the analyzed



183 particles were agglomerates of tar ball spheres, which suggest that weak diffusion limited  
184 collisional growth mechanism was involved in their formation process in the smoldering fire.  
185 Figure 2 shows the study-averaged mobility diameter number size distribution for the two fuels  
186 as measured by SMPS. For each fuel, it was observed that with increasing moisture content the  
187 total number concentration of the emitted particles decreased. Further, the median particle  
188 diameter for both fuel types was observed to decrease with increasing moisture content. For  
189 Alaskan peat burns, the study-averaged median particle diameters were 91 nm and 76 nm at 25%  
190 and 50% fuel moisture content, respectively, while for Siberian peat, the median diameters were  
191 136 nm and 109 nm at 25% and 50% fuel moisture content, respectively.

192 Figure 3 shows the wavelength dependence of the measured MAE values, connected by best-fit  
193 curves (cubic spline), for the emitted aerosols. For Siberian peat samples, MAE values lie in the  
194 range of 0.5-0.8 m<sup>2</sup>g<sup>-1</sup> at 405 nm and drop rapidly to 0.03-0.07 m<sup>2</sup>g<sup>-1</sup> at 532 nm. The MAE values  
195 at 405 nm for Alaskan peat are slightly lower, in the range of 0.2-0.5 m<sup>2</sup>g<sup>-1</sup>, and exhibit a similar  
196 rapid decline at 532 nm. The observed wavelength-varying MAE trends for both fuels are  
197 consistent with those observed for brown carbon (BrC) aerosols—a class of OC aerosols  
198 absorbing strongly in the near-UV wavelengths—emitted from biomass combustion burning  
199 (Chakrabarty et al., 2010; Hoffer et al., 2006; Kirchstetter and Thatcher, 2012). The low MAE  
200 values at 532 nm for both peat types compare well with those of Indonesian peat [*Chand et al.*,  
201 2005].

202 Fitting power-law functions to our measured MAE spectra between wavelengths  $\lambda = 405$  and 532  
203 nm yielded mean Absorption Ångström exponent  $\alpha$  values of 8.7 for both Siberian 25 and 50%  
204 fuel moisture content peat burns, and 7.7 and 10.8 for Alaskan 25% and 50% fuel moisture  
205 content peat burns, respectively.  $\alpha$  is an intensive optical property that characterizes the inherent

206 material property. For BC particles, typical values of  $\alpha \approx 1$  have been observed, while for BrC  
207 aerosols,  $\alpha$  ranges from 2 to higher values (Chakrabarty et al., 2010; Moosmuller et al., 2009).  
208 Compared with previously reported  $\alpha$  values for emissions from laboratory-combusted wildland  
209 fuels, emissions from peat burning characterized in this study displayed substantially higher  
210 values (Gyawali et al., 2009; Lack et al., 2012; Lewis et al., 2008b). It was also observed that  
211 with decreasing moisture content in the peat samples, the emitted aerosols exhibited higher  $\alpha$   
212 values. Over the 405-870 nm spectra, the average  $\alpha$  for both peat types were in the range of 4.9  
213 ( $\pm 0.75$ ) - 7.13 ( $\pm 0.88$ ). However, the trend for MAE values with varying levels of fuel moisture  
214 content was not very clear. With increasing moisture content, the MAE values of aerosols from  
215 Alaskan peat samples increased; while a decreasing trend was observed for aerosols from  
216 Siberian peat samples. A more detailed study on the optical characteristics of chromophores  
217 constituting both aerosol types might be necessary toward explanation this trend (Laskin et al.,  
218 2015). Such a study is beyond the scope of this current work.

219 The SSA values of the aerosol spanned a range of 0.92–1. They were consistently higher (0.99-  
220 1.00) at 532 and 781 nm than that at 405 nm for all peat samples irrespective of moisture content.  
221 This is likely due to the large proportion of BrC in all peat smoke aerosols that preferentially  
222 absorbs in the UV region thereby lowering SSA at 405 nm. The calculated SSA values compare  
223 well with previous laboratory studies for combustion of Indonesian peat samples [*Chand et al.*,  
224 2005] and from previous field measurements of peat smoke over Moldova [*Eck et al.*, 2003].

#### 225 **4 Impact on Direct Radiative Forcing**

226 We estimate the clear-sky direct radiative forcing per unit optical depth by the emitted BrC  
227 aerosols with the help of the “simple forcing efficiency” (SFE,  $W\ g^{-1}$ ) concept (Bond and  
228 Bergstrom, 2006). Most models assume that OC emitted from biomass combustion has net

229 negative forcing per gram of emitted aerosol (Bond et al., 2013). The wavelength-dependent SFE  
230 equation is given as:

$$231 \quad \frac{dSFE}{d\lambda} = -\frac{1}{4} \frac{dS(\lambda)}{d\lambda} \tau^2(\lambda)(1 - F_c)[2(1 - a_s)^2 \beta(\lambda) * MSE(\lambda) - 4a_s * MAE(\lambda)] \quad (1)$$

232 where  $dS(\lambda)/d\lambda$  is the solar irradiance,  $\tau$  is the atmospheric transmission (0.79),  $F_c$  is the cloud  
233 fraction (0.6),  $a$  is the surface albedo (0.19 for earth average and 0.8 for snow (Chen, 2011; Chen  
234 and Bond, 2010)),  $\beta$  is the fraction of scattered sunlight that is scattered into the upward  
235 hemisphere ( $\approx 0.17$  for biomass burning BrC aerosols), and MSE and MAE are the mass  
236 scattering and absorption efficiencies per gram, respectively (Chen and Bond, 2010; Griggs and  
237 Noguera, 2002; Saleh et al., 2014). Note that this equation doesn't account for hygroscopicity,  
238 which could affect SFE. Net forcing in the 405-880 nm spectral range was calculated by  
239 integrating the SFE equation using the tropospheric solar spectrum (Levinson et al., 2010).

240 Figure 4 a and b show forcing efficiencies at each wavelength over a bright surface (surface  
241 albedo of 0.8), which is characteristic of the snow-covered Arctic landscape and low-level clouds  
242 over which smoke plume typically moves. Integrated mean forcing over the solar spectrum is 20  
243 and 38 W g<sup>-1</sup> for BrC aerosols from Alaskan and Siberian peat burns, respectively. By assuming  
244 no absorption for the emitted aerosols, a convention often adopted by climate modelers while  
245 representing OC, we get a mean negative forcing of -3.7 and -5 W g<sup>-1</sup> for smoke from Alaskan  
246 and Siberian peat samples, respectively. These calculations were repeated for a surface albedo of  
247 0.19 (earth average (Chen and Bond, 2010)). The integrated forcing was negative in the visible  
248 wavelengths with mean values of -70 and -81 W g<sup>-1</sup> from Alaskan and Siberian peat samples,  
249 respectively. It is interesting to contrast and compare the extremely high integrated forcing value  
250 for BC over land, which is around 210 W/g (Chen, 2011).

251 Figure 5 a and b show net forcing efficiencies, integrated over the tropospheric solar spectrum,  
252 as a function of surface albedo ( $a_s$ ) for aerosols emitted from both fuel types. For Siberian peat  
253 samples, the forcing efficiency crosses over from negative (cooling) to positive (warming) values  
254 at  $a_s \approx 0.5$ . The cross-over points are nearly identical for varying fuel moisture content. However,  
255 for Alaskan peat with 50% moisture content, the cross-over takes place at a lower value ( $a_s \approx$   
256 0.57) compared to  $a_s \approx 0.61$  for 25% moisture content. Overall, these results suggest that BrC  
257 aerosols from boreal peatland burning could result in a net warming effect of the atmosphere  
258 only if they reside over bright surfaces with albedo greater than 0.6.

## 259 **5 Conclusions**

260 Our findings show that BrC aerosols from peatland fires in the Boreal region may give rise to  
261 significant absorption in the shorter visible wavelengths and the ultraviolet regions of the solar  
262 spectrum. This strong absorptivity may result in the positive net forcing (warming) over bright  
263 surfaces. The common understanding has been that BC constitutes the light-absorbing aerosol  
264 type from boreal forest fires (Randerson et al., 2006), while OC is light scattering in nature and  
265 helps offset the BC warming effects. However, our results show that aerosols containing BrC,  
266 which is a class of OC, could further amplify the warming effects of BC in this region, especially  
267 since 47% of incoming solar energy is distributed between 400 nm and 700 nm wavelengths.  
268 Additionally, absorption in the ultraviolet range by BrC aerosols could affect photolysis-driven  
269 atmospheric chemistry and consequently reduce tropospheric ozone concentration (Jacobson,  
270 1998).

271 **The Supplement related to this article is available online at**

272 **<http://dx.doi.org/10.5194/acpd-15-1-2015-supplement>**

## 273 **Acknowledgements**

274 This material is based upon work supported by the National Science Foundation under

275 Grant Nos. AGS1455215, DEB1342094, and DEB1354482; NASA ROSES under Grant Nos.  
276 NNX15AI66G and NNX15AI48G; NASA EPSCoR under Cooperative Agreement  
277 No. NNX14AN24A; and the Desert Research Institute's Wildland Fire Science Center (WFSC) and  
278 EDGES program.

279 **References**

- 280 Abu-Rahmah, A., Arnott, W. P., and Moosmüller, H.: Integrating Nephelometer with a Low  
281 Truncation Angle and an Extended Calibration Scheme, *Meas. Sci. Technol.*, 17, 1723-1732,  
282 2006.
- 283 Arnott, W. P., Moosmüller, H., Rogers, C. F., Jin, T., and Bruch, R.: Photoacoustic Spectrometer  
284 for Measuring Light Absorption by Aerosol: Instrument Description, *Atmos. Environ.*, 33, 2845-  
285 2852, 1999.
- 286 Bachelet, D., Lenihan, J., Neilson, R., Drapek, R., and Kittel, T.: Simulating the response of  
287 natural ecosystems and their fire regimes to climatic variability in Alaska, *Canadian Journal of*  
288 *Forest Research*, 35, 2244-2257, 2005.
- 289 Balshi, M. S., McGuire, A. D., Duffy, P., Flannigan, M., Kicklighter, D. W., and Melillo, J.:  
290 Vulnerability of carbon storage in North American boreal forests to wildfires during the 21st  
291 century, *Global Change Biology*, 15, 1491-1510, 2009.
- 292 Bonan, G. B.: Forests and climate change: forcings, feedbacks, and the climate benefits of  
293 forests, *Science*, 320, 1444-1449, 2008.
- 294 Bond, T. and Bergstrom, R.: Light Absorption by Carbonaceous Particles: An Investigative  
295 Review, *Aerosol Sci. Technol.*, 40, 27-67, 2006.
- 296 Bond, T., Doherty, S., Fahey, D., Forster, P., Berntsen, T., DeAngelo, B., Flanner, M., Ghan, S.,  
297 Kärcher, B., and Koch, D.: Bounding the role of black carbon in the climate system: a scientific  
298 assessment, *J. Geophys. Res.*, 118, 5380–5552, 2013.
- 299 Chakrabarty, R., Moosmüller, H., Chen, L., Lewis, K., Arnott, W., Mazzoleni, C., Dubey, M.,  
300 Wold, C., Hao, W., and Kreidenweis, S.: Brown carbon in tar balls from smoldering biomass  
301 combustion, *Atmos. Chem. Phys.*, 10, 6363-6370, 2010.
- 302 Chakrabarty, R., Moosmüller, H., Garro, M. A., Arnott, W. P., Walker, J., Susott, R. A., Babbitt,  
303 R. E., Wold, C. E., Lincoln, E. N., and Hao, W. M.: Emissions from the laboratory combustion  
304 of wildland fuels: Particle morphology and size, *J. Geophys. Res.*, 111, D07204, 2006.
- 305 Chen, L. W. A., Moosmüller, H., Arnott, W. P., Chow, J. C., Watson, J. G., Susott, R. A.,  
306 Babbitt, R. E., Wold, C. E., Lincoln, E. N., and Hao, W. M.: Emissions from laboratory  
307 combustion of wildland fuels: Emission factors and source profiles, *Environ. Sci. Technol.*, 41,  
308 4317-4325, 2007.
- 309 Chen, Y.: Characterization of carbonaceous aerosols from biofuel combustion: emissions and  
310 climate relevant properties, Doctoral Dissertation, University of Illinois Urbana Champaign,  
311 Illinois Digital Environment for Access to Learning and Scholarship, 215 pp., 2011.
- 312 Chen, Y. and Bond, T.: Light absorption by organic carbon from wood combustion, *Atmos.*  
313 *Chem. Phys.*, 10, 1773-1787, 2010.
- 314 Chow, J. C., Watson, J. G., Chen, L.-W. A., Chang, M. O., Robinson, N. F., Trimble, D., and  
315 Kohl, S.: The IMPROVE\_A temperature protocol for thermal/optical carbon analysis:  
316 Maintaining consistency with a long-term database, *J. Air Waste Manage. Assoc.*, 57, 1014-  
317 1023, 2007.

318 Chow, J. C., Watson, J. G., Robles, J., Wang, X., Chen, L.-W. A., Trimble, D. L., Kohl, S. D.,  
319 Tropp, R. J., and Fung, K. K.: Quality assurance and quality control for thermal/optical analysis  
320 of aerosol samples for organic and elemental carbon, *Anal. Bioanal. Chem.*, 401, 3141-3152,  
321 2011.

322 Christian, T. J., Kleiss, B., Yokelson, R. J., Holzinger, R., Crutzen, P., Hao, W. M., Saharjo, B.,  
323 and Ward, D. E.: Comprehensive laboratory measurements of biomass-burning emissions: 1.  
324 Emissions from Indonesian, African, and other fuels, *Journal of Geophysical Research:*  
325 *Atmospheres* (1984–2012), 108, 2003.

326 Chung, C. E., Ramanathan, V., and Decremer, D.: Observationally constrained estimates of  
327 carbonaceous aerosol radiative forcing, *Proceedings of the National Academy of Sciences*, 109,  
328 11624-11629, 2012.

329 Conard, S. G. and Ivanova, G. A.: Wildfire in Russian boreal forests—Potential impacts of fire  
330 regime characteristics on emissions and global carbon balance estimates, *Environ. Pollut.*, 98,  
331 305-313, 1997.

332 Eck, T., Holben, B., Reid, J., Sinyuk, A., Hyer, E., O'Neill, N., Shaw, G., Vande Castle, J.,  
333 Chapin, F., and Dubovik, O.: Optical properties of boreal region biomass burning aerosols in  
334 central Alaska and seasonal variation of aerosol optical depth at an Arctic coastal site, *Journal of*  
335 *Geophysical Research: Atmospheres* (1984–2012), 114, 2009.

336 Flannigan, M. D., Logan, K. A., Amiro, B. D., Skinner, W. R., and Stocks, B.: Future area  
337 burned in Canada, *Climatic change*, 72, 1-16, 2005.

338 Gorham, E.: The future of research in Canadian peatlands: a brief survey with particular  
339 reference to global change, *Wetlands*, 14, 206-215, 1994.

340 Griggs, D. J. and Noguer, M.: Climate change 2001: the scientific basis. Contribution of working  
341 group I to the third assessment report of the intergovernmental panel on climate change,  
342 *Weather*, 57, 267-269, 2002.

343 Gustafsson, O., Krusa, M., Zencak, Z., Sheesley, R. J., Granat, L., Engstrom, E., Praveen, P. S.,  
344 Rao, P. S. P., Leck, C., and Rodhe, H.: Brown Clouds over South Asia: Biomass or Fossil Fuel  
345 Combustion?, *Science*, 323, 495-498, 2009.

346 Gyawali, M., Arnott, W., Lewis, K., and Moosmüller, H.: In situ aerosol optics in Reno, NV,  
347 USA during and after the summer 2008 California wildfires and the influence of absorbing and  
348 non-absorbing organic coatings on spectral light absorption, *Atmos. Chem. Phys.*, 9, 8007-8015,  
349 2009.

350 Hoffer, A., Gelencsér, A., Guyon, P., Kiss, G., Schmid, O., Frank, G., Artaxo, P., and Andreae,  
351 M.: Optical properties of humic-like substances (HULIS) in biomass-burning aerosols, *Atmos.*  
352 *Chem. Phys.*, 6, 3563-3570, 2006.

353 Hu, F. S., Higuera, P. E., Walsh, J. E., Chapman, W. L., Duffy, P. A., Brubaker, L. B., and  
354 Chipman, M. L.: Tundra burning in Alaska: linkages to climatic change and sea ice retreat,  
355 *Journal of Geophysical Research: Biogeosciences* (2005–2012), 115, 2010.

356 Inuma, Y., Brüggemann, E., Gnauk, T., Müller, K., Andreae, M., Helas, G., Parmar, R., and  
357 Herrmann, H.: Source characterization of biomass burning particles: The combustion of selected

358 European conifers, African hardwood, savanna grass, and German and Indonesian peat, *Journal*  
359 *of Geophysical Research: Atmospheres* (1984–2012), 112, 2007.

360 Jacobson, M. Z.: Studying the effects of aerosols on vertical photolysis rate coefficient and  
361 temperature profiles over an urban airshed, *Journal of Geophysical Research: Atmospheres*  
362 (1984–2012), 103, 10593-10604, 1998.

363 Jorgenson, M. T., Racine, C. H., Walters, J. C., and Osterkamp, T. E.: Permafrost degradation  
364 and ecological changes associated with a warming climate in central Alaska, *Climatic change*, 48,  
365 551-579, 2001.

366 Kirchstetter, T. and Thatcher, T.: Contribution of organic carbon to wood smoke particulate  
367 matter absorption of solar radiation, *Atmos. Chem. Phys*, 12, 6067-6072, 2012.

368 Lack, D. A., Langridge, J. M., Bahreini, R., Cappa, C. D., Middlebrook, A. M., and Schwarz, J.  
369 P.: Brown carbon and internal mixing in biomass burning particles, *Proc. Natl. Acad. Sci. U. S.*  
370 *A.*, 109, 14802-14807, 2012.

371 Laskin, A., Laskin, J., and Nizkorodov, S. A.: Chemistry of Atmospheric Brown Carbon, *Chem.*  
372 *Rev.* (Washington, DC, U. S.), 115, 4335-4382, 2015.

373 Lawrence, D. M. and Slater, A. G.: A projection of severe near-surface permafrost degradation  
374 during the 21st century, *Geophys. Res. Lett.*, 32, 2005.

375 Levinson, R., Akbari, H., and Berdahl, P.: Measuring solar reflectance—Part I: Defining a metric  
376 that accurately predicts solar heat gain, *Solar Energy*, 84, 1717-1744, 2010.

377 Lewis, K., Arnott, W. P., Moosmuller, H., and Wold, C. E.: Strong spectral variation of biomass  
378 smoke light absorption and single scattering albedo observed with a novel dual-wavelength  
379 photoacoustic instrument, *J. Geophys. Res.*, 113, doi:10.1029/2007JD009699, 2008a.

380 Lewis, K., Arnott, W. P., Moosmüller, H., and Wold, C. E.: Strong spectral variation of biomass  
381 smoke light absorption and single scattering albedo observed with a novel dual-wavelength  
382 photoacoustic instrument, *Journal of Geophysical Research: Atmospheres* (1984–2012), 113,  
383 2008b.

384 Moosmuller, H., Chakrabarty, R. K., and Arnott, W. P.: Aerosol light absorption and its  
385 measurement: A review, *J. Quant. Spectrosc. Radiat. Transfer*, 110, 844-878, 2009.

386 Oris, F., Asselin, H., Ali, A. A., Finsinger, W., and Bergeron, Y.: Effect of increased fire activity  
387 on global warming in the boreal forest, *Environmental Reviews*, 22, 206-219, 2013.

388 Page, S., Wüst, R., Weiss, D., Rieley, J., Shotyk, W., and Limin, S. H.: A record of Late  
389 Pleistocene and Holocene carbon accumulation and climate change from an equatorial peat bog  
390 (Kalimantan, Indonesia): implications for past, present and future carbon dynamics, *Journal of*  
391 *Quaternary Science*, 19, 625-635, 2004.

392 Page, S. E., Siegert, F., Rieley, J. O., Boehm, H. D. V., Jaya, A., and Limin, S.: The amount of  
393 carbon released from peat and forest fires in Indonesia during 1997, *Nature*, 420, 61-65, 2002.

394 Pearson, R. G., Phillips, S. J., Lorant, M. M., Beck, P. S., Damoulas, T., Knight, S. J., and  
395 Goetz, S. J.: Shifts in Arctic vegetation and associated feedbacks under climate change, *Nature*  
396 *Climate Change*, 3, 673-677, 2013.



397 Pósfai, M., Simonics, R., Li, J., Hobbs, P. V., and Buseck, P. R.: Individual Aerosol Particles  
398 from Biomass Burning in Southern Africa: 1. Compositions and Size Distributions of  
399 Carbonaceous Particles, *Journal of Geophysical Research*, 108, DOI:10.1029/2002JD002291,  
400 2003.

401 Randerson, J. T., Liu, H., Flanner, M. G., Chambers, S. D., Jin, Y., Hess, P. G., Pfister, G.,  
402 Mack, M., Treseder, K., and Welp, L.: The impact of boreal forest fire on climate warming,  
403 *Science*, 314, 1130-1132, 2006.

404 Rein, G., Cleaver, N., Ashton, C., Pironi, P., and Torero, J. L.: The severity of smouldering peat  
405 fires and damage to the forest soil, *Catena*, 74, 304-309, 2008.

406 Saleh, R., Robinson, E. S., Tkacik, D. S., Ahern, A. T., Liu, S., Aiken, A. C., Sullivan, R. C.,  
407 Presto, A. A., Dubey, M. K., and Yokelson, R. J.: Brownness of organics in aerosols from  
408 biomass burning linked to their black carbon content, *Nat. Geosci.*, 2014. 2014.

409 Sheng, Y., Smith, L. C., MacDonald, G. M., Kremenetski, K. V., Frey, K. E., Velichko, A. A.,  
410 Lee, M., Beilman, D. W., and Dubinin, P.: A high-resolution GIS-based inventory of the west  
411 Siberian peat carbon pool, *Global Biogeochem. Cycles*, 18, 2004.

412 Simpson, I. J., Akagi, S., Barletta, B., Blake, N., Choi, Y., Diskin, G., Fried, A., Fuelberg, H.,  
413 Meinardi, S., and Rowland, F.: Boreal forest fire emissions in fresh Canadian smoke plumes: C  
414 1-C 10 volatile organic compounds (VOCs), CO<sub>2</sub>, CO, NO<sub>2</sub>, NO, HCN and CH<sub>3</sub>CN, *Atmos.*  
415 *Chem. Phys.*, 11, 6445-6463, 2011.

416 Solomon, S., Qin, D., Manning, M., Chen, Z., Marquis, M., Averyt, K., Tignor, M., and Miller,  
417 H.: The physical science basis, Contribution of working group I to the fourth assessment report  
418 of the intergovernmental panel on climate change, 2007. 235-337, 2007.

419 Stocker, T. F., Dahe, Q., and Plattner, G.-K.: Climate Change 2013: The Physical Science Basis,  
420 Working Group I Contribution to the Fifth Assessment Report of the Intergovernmental Panel on  
421 Climate Change. Summary for Policymakers (IPCC, 2013), 2013. 2013.

422 Stocks, B. J., Fosberg, M., Lynham, T., Mearns, L., Wotton, B., Yang, Q., Jin, J., Lawrence, K.,  
423 Hartley, G., and Mason, J.: Climate change and forest fire potential in Russian and Canadian  
424 boreal forests, *Climatic change*, 38, 1-13, 1998.

425 Stockwell, C., Yokelson, R., Kreidenweis, S., Robinson, A., DeMott, P., Sullivan, R., Reardon,  
426 J., Ryan, K., Griffith, D. W., and Stevens, L.: Trace gas emissions from combustion of peat, crop  
427 residue, domestic biofuels, grasses, and other fuels: configuration and Fourier transform infrared  
428 (FTIR) component of the fourth Fire Lab at Missoula Experiment (FLAME-4), 2014. 2014.

429 Tian, J., Chow, J. C., Cao, J., Han, Y., Ni, H., Chen, L.-W. A., Wang, X., Huang, R.,  
430 Moosmüller, H., and Watson, J. G.: A Biomass Combustion Chamber: Design, Evaluation, and a  
431 Case Study of Wheat Straw Combustion Emission Tests, *Aerosol and Air Quality Research*, 15,  
432 2104-2114, 2015.

433 Turetsky, M. R., Benscoter, B., Page, S., Rein, G., van der Werf, G. R., and Watts, A.: Global  
434 vulnerability of peatlands to fire and carbon loss, *Nat. Geosci.*, 8, 11-14, 2015.

435 Ward, D. E., Hao, W. M., Susott, R. A., Babbitt, R. E., Shea, R. W., Kauffman, J. B., and Justice,  
436 C. O.: Effect of fuel composition on combustion efficiency and emission factors for African  
437 savanna ecosystems, *J. Geophys. Res.*, 101, 23569-23576, 1996.

438 Xu, R., Ferrante, L., Briens, C., and Berruti, F.: Bio-oil production by flash pyrolysis of  
439 sugarcane residues and post treatments of the aqueous phase, *J. Anal. Appl. Pyrolysis*, 91, 263-  
440 272, 2011.

441

442

**Table 1:** Mean mass-based emission factors (rounded to nearest integer) of carbonaceous gases and aerosols from emissions of Alaskan and Siberian peat in this study.

Fuel Type	Fuel Moisture Content	Mean Fuel-Based Emission Factors (g kg <sup>-1</sup> fuel)			
		CO <sub>2</sub>	CO	OC	BC
Alaskan Peat	25%	1238	83	7	0.1
Alaskan Peat	50%	1598	128	4	0.2
Siberian Peat	25%	1432	204	17	0.2
Siberian Peat	50%	1698	49	11	0.1

**Figure 1:** Transmission electron microscopy (TEM) images of typical organic carbon "tar balls", occurring as spheres and agglomerates, emitted from smoldering combustion of Alaskan and Siberian peat samples. The internal structure of these particles were was amorphous in nature. Electron dispersive spectroscopy (EDX) of tar balls shows that these particles consist primarily of carbon and oxygen with an average molar ratio of ranging between 6-7.

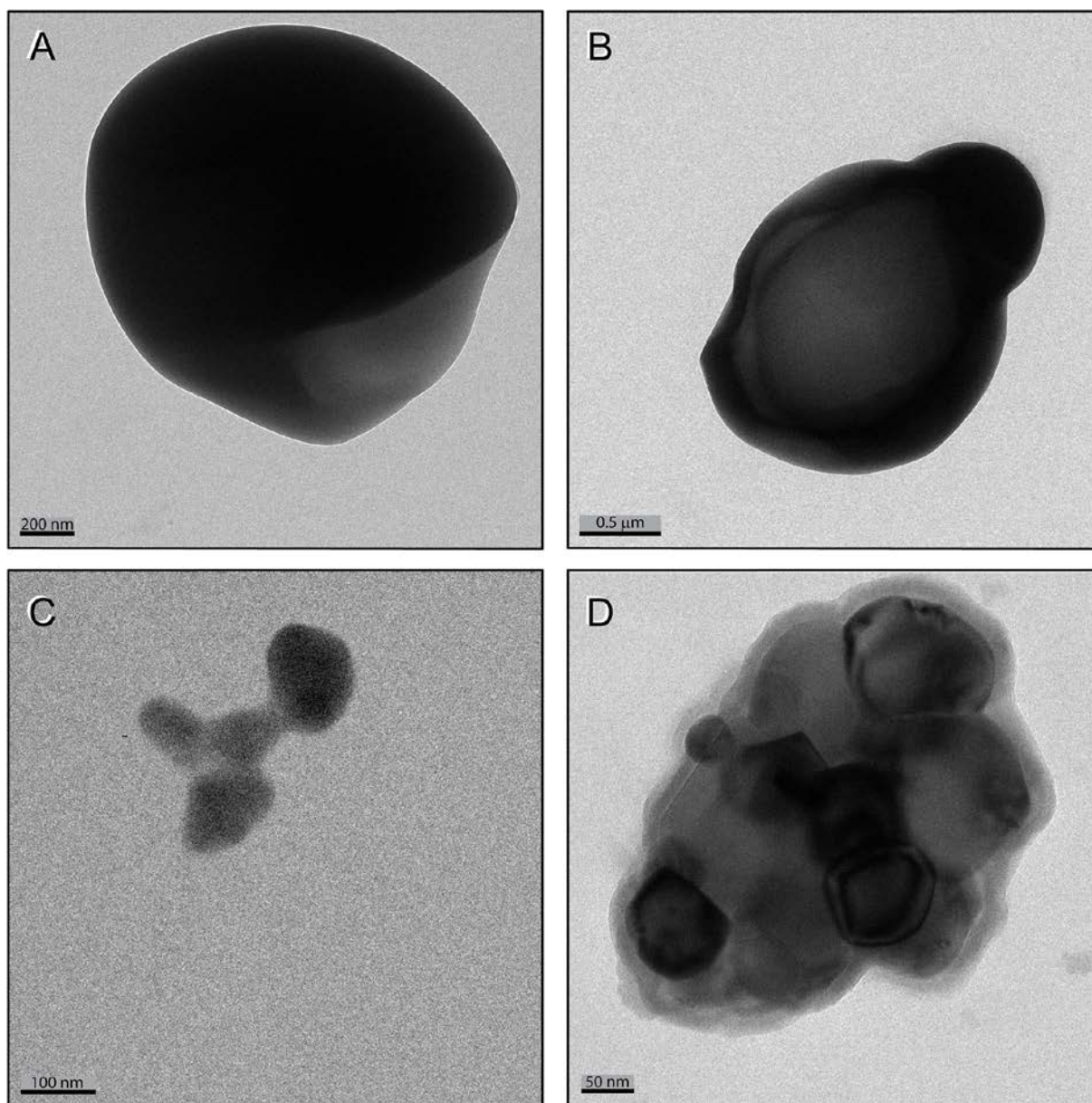


**Figure 2:** Study-averaged mobility number size distribution of aerosols from Alaskan and Siberian peat samples.

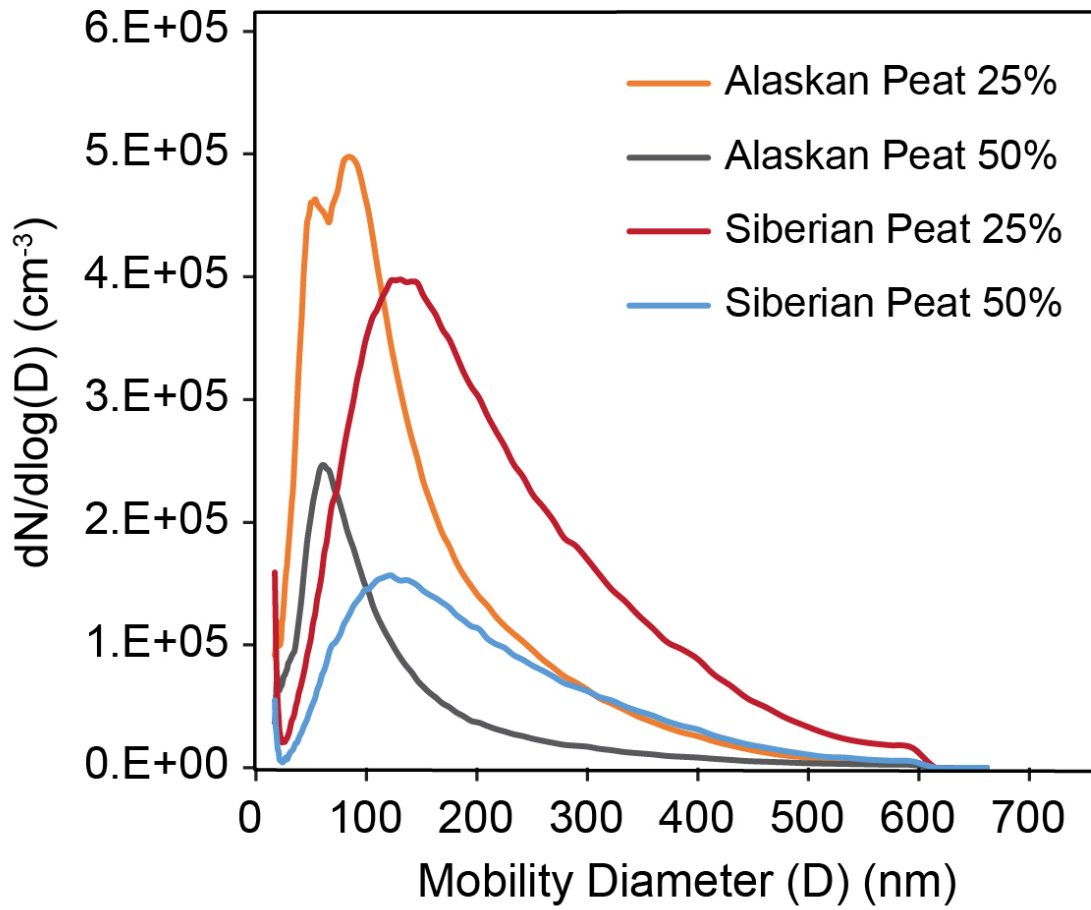


**Figure 3:** Wavelength-dependent mass absorption efficiency (MAE) of the sampled carbonaceous (brown) aerosols from (A) Alaskan and (B) Siberian peat smoldering combustion. The dashed lines show study-averaged values. The shaded bands correspond to error bars measured at 405, 532, 781, and 870 nm, and connected by best-fit curves.

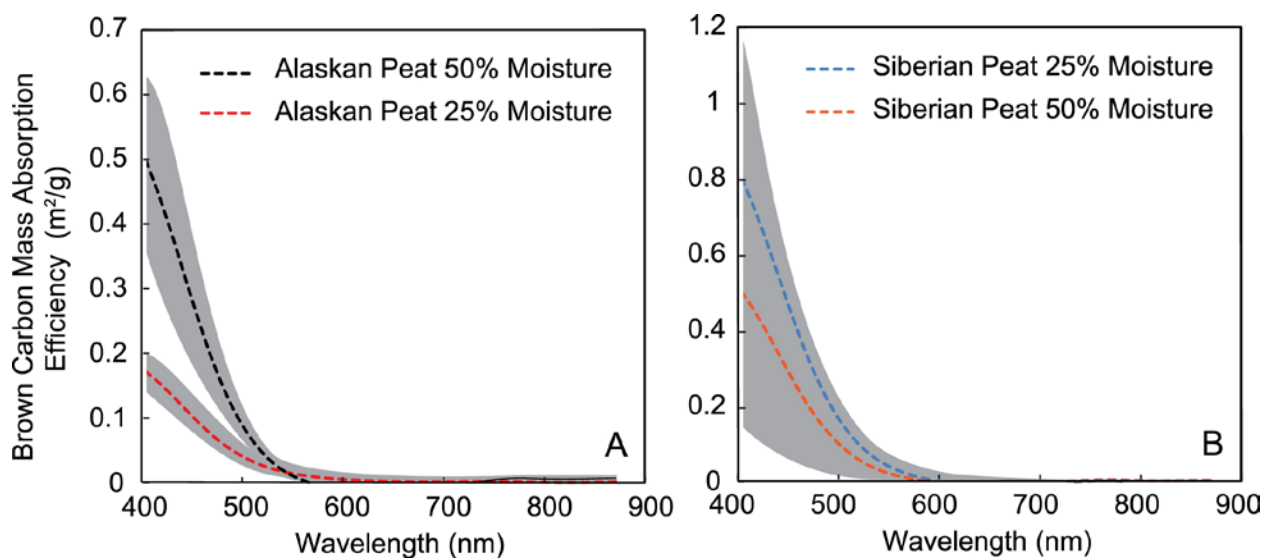
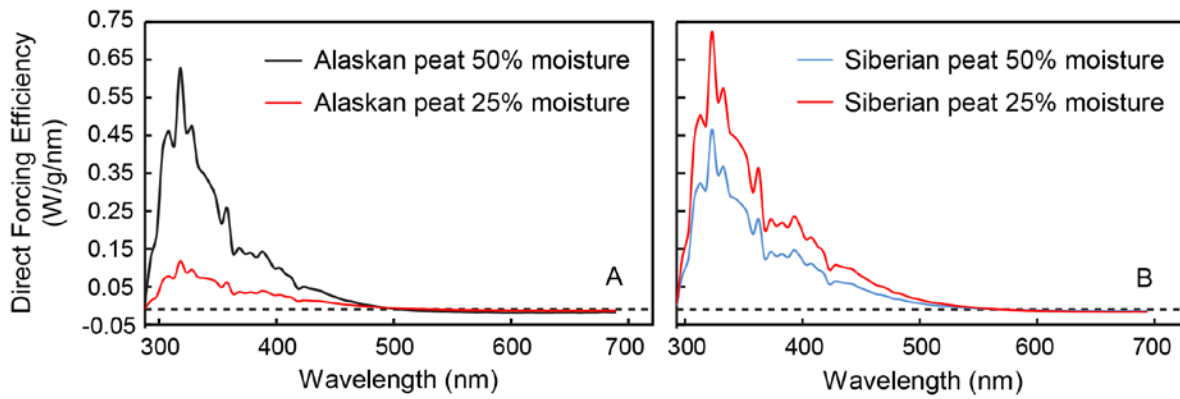


**Figure 4:** Direct forcing efficiency of brown carbon aerosols above snow (surface albedo = 0.8). Integrated mean forcing is 20 and 38 W g<sup>-1</sup> for Alaskan and Siberian peat smoke aerosols, respectively.



443

**Figure 5:** Net forcing efficiencies as a function of surface albedo for Siberian and Alaskan peat smoke aerosols. The cross-over from negative (cooling) to positive (warming) values takes place between surface albedo values of 0.55 – 0.6.

